

PLANT SCIENCES

Haploid induction by a maize *cenh3* null mutantNa Wang¹, Jonathan I. Gent¹, R. Kelly Dawe^{1,2*}

The production of haploids is an important first step in creating many new plant varieties. One approach used in *Arabidopsis* involves crossing plants expressing different forms of centromeric histone H3 (CENP-A/CENH3) and subsequent loss of genome with weaker centromeres. However, the method has been ineffective in crop plants. Here, we describe a greatly simplified method based on crossing maize lines that are heterozygous for a *cenh3* null mutation. Crossing *+cenh3* to wild-type plants in both directions yielded haploid progeny. Genome elimination was determined by the *cenh3* genotype of the gametophyte, suggesting that centromere failure is caused by CENH3 dilution during the postmeiotic cell divisions that precede gamete formation. The *cenh3* haploid inducer works as a vigorous hybrid and can be transferred to other lines in a single cross, making it versatile for a variety of applications.

INTRODUCTION

Tens of thousands of maize haploid lines are generated by breeding companies around the world each year as a prerequisite for creating new inbreds, which are ultimately used to produce hybrids for sale. The induced haploids are doubled by colchicine and immediately tested for agronomic performance. The traditional technology is based on an inbred called Stock 6 that induces haploids when crossed as a male (1) and, in modern lines, has been reported to induce haploids at frequencies as high as ~15% (2). The key underlying gene, called *Matrilineal* (MATL/ZMPLA1/NLD), is a patatin-like phospholipase expressed primarily in pollen (3–5). Its mechanism of action is not understood but may involve a change in membrane properties during fertilization that leads to a loss of the paternal chromosomes. Mutations in *matrilineal* also induce haploids in rice and wheat (6–8). The *Matrilineal* gene is not conserved in dicotyledonous plants, although recent work has revealed a conserved enhancer of *matrilineal* that induces haploids at low levels in *Arabidopsis* (9).

A potentially superior and broadly useful method of inducing haploids was pioneered by Ravi and Chan (10), who showed that crossing *Arabidopsis* lines with a structurally altered centromeric histone H3 (CENP-A/CENH3) protein yielded haploids and aneuploids at frequencies as high as 25 to 45%. CENP-A, called CENH3 in plants, is a histone variant that recruits constitutive centromere proteins that subsequently recruit overlying kinetochore proteins (11–14). The original study involved a construct called *GFP-tailswap* where the N-terminal tail of CENH3 was replaced with sequence from another H3 variant and modified with a green fluorescent protein (GFP) tag. Recent data demonstrate that point mutations and small deletions of CENH3 can also induce haploids at similar frequencies (15–17). However, outside of *Arabidopsis*, centromere-mediated haploid induction has proven to be less effective, generally producing <1% haploids (18).

In an earlier report, we proposed that the mechanism of centromere-mediated haploid induction is based on differences in effective centromere size between haploid inducers and their wild-type crossing partners (19). *CENH3* point mutations reduce CENH3 loading in somatic cells (15), and *GFP-tailswap* lines show impaired CENH3 loading in meiosis (20), suggesting that haploid inducers transmit

small or weak centromeres to gametophytes. When crossed to wild-type plants, the progeny have a centromere size imbalance, which we argued leads to targeted destruction of the smaller centromeres by natural clearing mechanisms that remove misplaced CENH3 and spurious small centromeres (19). The centromere size model predicts that *cenh3* mutants with the most severe loss of function will be the best haploid inducers. However, severe *cenh3* mutants also compromise plant growth, making it difficult to breed a healthy haploid inducer line. This contradiction in goals likely explains the poor success record of centromere-mediated haploid induction in species other than *Arabidopsis*.

RESULTS

The current study was designed to test the centromere size model in maize, initially using the *GFP-tailswap* method. However, this approach is complicated by the fact that it requires both a mutant of native *cenh3* and a functional *GFP-tailswap* transgene that complements the mutant. Another group had already shown some success using an existing maize mutant (*cenh3-mu1015598*) caused by a Robertson's *Mutator* (*Mu*) insertion in the 5' untranslated region (5'UTR) of the gene (21, 22). They crossed *GFP-tailswap* into the *cenh3-mu1015598* background and observed an average of 0.86% haploids when crossed as a male and no haploids when crossed as a female (21). We also obtained *cenh3-mu1015598* and self-crossed three heterozygous plants. Genotyping revealed that two ears segregated a low frequency of homozygous mutants that grew to various states of maturity (table S1). The recovery of homozygous mutants indicates that *cenh3-mu1015598* is not a null and that prior results may have been confounded by a low level of wild-type *CENH3* expression. The variable penetrance of the *cenh3-mu1015598* allele can be explained by the fact that *Mu* elements can promote low levels of expression when inserted into 5'UTR regions (23).

To overcome the selection against true null *cenh3* alleles, we opted to create a *cenh3* null using a two-construct CRISPR-Cas9 approach. One line was transformed with a simple construct expressing Cas9 driven by an ubiquitin promoter. A second line was transformed with a construct expressing a guide RNA (gRNA) targeting the native *CENH3* gene and an “*ImmuneCENH3*” gene that contains a full-length native *CENH3* gene with five silent nucleotide changes in the gRNA target area (Fig. 1, A and B). After we crossed the two lines together, Cas9 generated mutations in the native *CENH3* gene

Copyright © 2021
The Authors, some
rights reserved;
exclusive licensee
American Association
for the Advancement
of Science. No claim to
original U.S. Government
Works. Distributed
under a Creative
Commons Attribution
NonCommercial
License 4.0 (CC BY-NC).

¹Department of Plant Biology, University of Georgia, Athens, GA 30602, USA. ²Department of Genetics, University of Georgia, Athens, GA 30602, USA.

*Corresponding author. Email: kdawe@uga.edu

but left the transgene unaffected. We chose a *cenh3* allele with a single-nucleotide deletion that causes a stop codon in the α N helix that connects the N-terminal tail to the inner nucleosome core particle (Fig. 1C). In the presence of *ImmuneCENH3*, the *cenh3* muta-

tion segregates as a simple Mendelian recessive trait (Table 1). We then created transgenics with *TailswapCENH3*, a close replica of the *Arabidopsis* *GFP-tailswap* construct, and crossed it to the *cenh3* mutation. We were unable to obtain any plants that contained *TailswapCENH3* and were homozygous for *cenh3* (Table 1), suggesting that the transgene does not complement a true null. This is likely because the GFP tag interferes with CENH3 loading or recruitment of other centromere proteins. *Arabidopsis* *GFP-tailswap* plants are severely stunted (24) and nearly sterile (20), indicating a similar negative impact. However, this may not prove to be true in all cases since, in animals, the function of CENP-A seems less affected by GFP or other large tags [e.g., (25, 26)].

During the course of these studies, we noted that *cenh3* was occasionally transmitted in the absence of *ImmuneCENH3*. By crossing to wild-type lines, we were able to obtain a simple segregating *cenh3* line that lacked both of the original transgenes. Among selfed progeny from a $+/\textit{cenh3}$ line, there were 163 $+/+$ wild-type individuals, 55 $+/\textit{cenh3}$ heterozygotes, and 0 *cenh3/cenh3* homozygotes, indicating that the mutant is homozygous, lethal and poorly transmitted through gametophytes. We also carried out reciprocal crosses between $+/\textit{cenh3}$ heterozygotes and wild-type plants. A Mendelian trait is normally transmitted to 50% of testcross progeny; however, we observed that only 12.1% of the progeny received *cenh3* when crossed through the male and 25% when crossed through the female (Table 2). The reduction in transmission is expected because sperm and eggs are carried within multicellular haploid gametophytes. Two haploid cell divisions precede the formation of an egg. Those gametophytes with the *cenh3* allele must use CENH3 carried over from the sporophytic phase while it is naturally diluted at each cell cycle (27). A general expectation is that *cenh3* sperm would have about one-quarter of the normal amount of CENH3 and an egg carrying *cenh3* would have about one-eighth relative to the *cenh3* heterozygous parent. Assuming no dosage compensation, those values would be reduced by an additional one-half relative to a normal homozygous wild-type parent. As a result, sperm and eggs carrying *cenh3* presumably have smaller centromeres.

To test whether $+/\textit{cenh3}$ heterozygous mutants are able to induce haploids, we crossed *cenh3* heterozygotes with tester lines in both directions. In the first test, we crossed wild-type and $+/\textit{cenh3}$ plants to a line that is homozygous for a recessive *glossy8* (*gl8*) mutation on

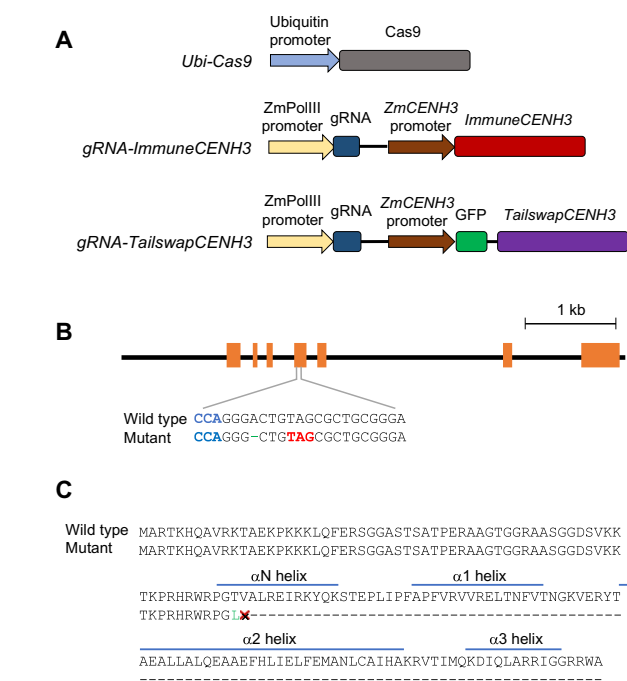


Fig. 1. Generation of a maize *cenh3* null mutation by CRISPR-Cas9. (A) Constructs used. Ubi-Cas9 includes a codon-optimized Cas9 driven by the maize polyubiquitin promoter. gRNA-*ImmuneCENH3* includes a gRNA targeting the fourth exon of *CENH3* and an uncleavable *ImmuneCENH3* gene driven by 2.2 kb of the *CENH3* native promoter. *TailswapCENH3* is based on *ImmuneCENH3* but includes a modified N-terminal tail and a GFP tag. (B) The maize *CENH3* gene showing the sequence targeted for gene editing. Exons are shown as orange boxes. The protospacer adjacent motif (in blue) and 20-base pair (bp) target sequence of the gRNA are shown, in both the wild-type and mutant forms. The mutant is a single base pair deletion that causes a stop codon (red). (C) Predicted protein sequence of the wild-type and mutant CENH3 protein. The stop codon occurs at the third position of the α N helix. This truncated protein may interact with DNA on the outer surface of the nucleosome but lacks the sequence that mediates the interaction with other histones inside the nucleosome core particle.

Table 1. Segregation of <i>cenh3</i> in <i>ImmuneCENH3</i> and <i>TailswapCENH3</i> backgrounds. The number of plants of each genotype are shown in parentheses.		
Cross	Transgene genotypes	<i>cenh3</i> genotypes
$+/\textit{ImmuneCENH3}$, $+/\textit{cenh3}$ ♂	$+/\textit{ImmuneCENH3}$ or <i>ImmuneCENH3/ImmuneCENH3</i>	$+/+$ (54)
	(172)	$+/\textit{cenh3}$ (75)
		<i>cenh3/cenh3</i> (43)
	$+/+$ (33)	
$+/\textit{TailswapCENH3}$, $+/\textit{cenh3}$ ♂	$+/\textit{TailswapCENH3}$ or <i>TailsCENH3/TailswapCENH3</i>	$+/+$ (47)
	(53)	$+/\textit{cenh3}$ (6)
		<i>cenh3/cenh3</i> (0)
	$+/+$ (16)	

chromosome 5 that causes seedling leaves to have a shiny appearance. We observed that 0.5% of the progeny were glossy when *+cenh3* heterozygotes were crossed as male and 5.0% of the progeny were glossy when *+cenh3* plants were crossed as female (Table 3). Flow cytometry analysis revealed that all 45 of the glossy plants were haploids, an interpretation that was confirmed by counting chromosomes in root tip cells of three plants (Fig. 2, A and B). When grown to maturity, the haploid plants were short and sterile as expected (Fig. 2, C and D) (28). We also observed two nonglossy plants with stunted phenotypes that we hypothesized might be aneuploids. These two plants were skim sequenced along with six haploids. While the haploids showed uniform sequence coverage, the stunted plants did not; one was trisomic for chromosome 3, and the other was monosomic for chromosomes 2 and 4 and trisomic for chromosome 10 (fig. S1).

We then carried out a second set of tests using *gl1*, which has a similar phenotype but the mutation is on chromosome 7. In these crosses, we also scored the germination rate, which is an indirect measure of karyotypic abnormality commonly used to estimate the efficacy of *Arabidopsis* haploid inducers (16, 29). In crosses where *+cenh3* heterozygotes were the female, 5.2% of the progeny were glossy and haploid by flow cytometry measurements. Another 3.3% of the progeny showed the glossy phenotype but had a higher DNA content than expected for haploids and were scored as aneuploids (Table 3 and table S2). Different crosses differed considerably in the germination rate (65 to 91%), frequencies of haploids (1.2 to 8.9%), and aneuploids (2.1 to 5.1%) (table S2). Sequence data from five aneuploid plants confirmed that all except one were missing chromosome 7, sometimes in conjunction with the loss of other chromosomes. One glossy plant that appeared to have two complete copies of chromosome 7 may have had a small interstitial deletion that was not detectable by skim sequencing [segmental aneuploids are common in *Arabidopsis GFP-tailswap* crosses (30)]. The results from the *gl1* tests are more in line with what has been observed in *Arabidopsis*,

where any given cross with *GFP-tailswap* generally yields haploids and aneuploids in similar proportions (10, 24, 29).

If CENH3 dilution is the underlying mechanism for haploid induction, then only gametes carrying the *cenh3* mutation from the *+cenh3* parent should induce haploids. Unfortunately, it is not possible to score seedlings for the presence of the *cenh3* allele because the genome of the haploid inducer is lost. However, data from *Arabidopsis GFP-tailswap* crosses show that endosperm rarely displays complete uniparental genome elimination when the seedling is haploid (29). If true in maize as well, then the genotype of the endosperm could be used to determine the original genotype of the seedling. We genotyped the remnant endosperm from a set of 11 haploid plants produced from a *+cenh3* × *gl8* cross. All 11 were heterozygous for the *cenh3* allele, indicating that haploid induction is caused by gametes carrying *cenh3*. Since only 25% of the progeny from a female cross receive *cenh3* (Table 2), yet our haploid frequencies are calculated on the basis of total seed counts, the effective haploid induction frequency is on the order of 20%. Bringing this level of haploid induction into practice will require screening for kernels that received *cenh3*. There are multiple publicly available endosperm-expressed GFP transgenes within 100 kb of the *CENH3* gene that could be linked to the null for this purpose (31) (www.acdsinsertions.org/).

DISCUSSION

We have described a highly simplified haploid induction system that is based on crossing plants heterozygous for a *cenh3* null mutation. The data suggest that CENH3 is diluted to critically low levels during the cell divisions of *cenh3* gametophytes and that the comparatively small centromeres are selectively degraded, leaving only the chromosomes from the crossing partner. Our work builds on the classic *GFP-tailswap* studies and recent improvements (10, 15, 17, 24, 32), as well as earlier work describing crosses between divergent plant species (often differing in centromere size) (19, 32) that result in

Table 2. Transmission of *cenh3* through male and female crosses. WT, wild type; het, *+cenh3* heterozygote; hom, *cenh3/cenh3* homozygote..

Cross	No. seedlings	Expected (WT:het:hom)	Observed (WT:het:hom)	Observed het frequency
<i>+cenh3</i> ♂	218	55:108:55	163:55:0	25.2%
<i>+cenh3</i> ♀ × B73 ♂	184	92:92:0	138:46:0	25.0%
B73 ♀ × <i>+cenh3</i> ♂	140	70:70:0	123:17:0	12.1%

Table 3. Haploid and aneuploid induction by *+cenh3* heterozygotes.

Cross	No. seedlings	No. glossy plants	No. haploid	Haploid ratio	No. aneuploid	Aneuploid ratio
<i>+cenh3</i> ♀ × <i>gl8</i> ♂	838	42	42	5.0%	2*	0.2%
WT ♀ × <i>gl8</i> ♂	1000	0	–	–	–	–
<i>gl8</i> ♀ × <i>+cenh3</i> ♂	597	3	3	0.5%	0	0
<i>gl8</i> ♀ × WT ♂	826	0	–	–	–	–
<i>+cenh3</i> ♀ × <i>gl1</i> ♂	844	75	44	5.2%	28	3.3%
WT ♀ × <i>gl1</i> ♂	1114	0	–	–	–	–

*The two aneuploid plants were nonglossy plants with stunted phenotypes.

centromere failure, haploidization, and reproductive isolation. Similar principles have emerged from the animal literature, where variation in centromere repeats can affect the quantity of CENP-A and skew meiotic transmission (33, 34) in a process known as centromere drive (35). Centromere drive is a form of genetic conflict that is hypothe-

sized to result in rapid evolution of both centromere repeats and associated centromere proteins (35, 36) and, in principle, can lead to centromere-based incompatibilities of the type observed with crosses involving different plant species. A central theme is that modifications to the quantity and/or quality of CENP-A/CENH3 can lead to postzygotic incompatibility, which, in plants, often results in haploid formation.

All prior literature on centromere-mediated haploid induction in plants describes the complementation of a null allele with structural variants of CENH3 or alleles that produce altered or partially deleted forms of CENH3 (10, 15, 17, 24, 32). These data have served to sustain the original interpretation that haploid induction is caused by a competition between two structurally different forms of CENH3 and ultimate rejection of the altered centromeres by a surveillance mechanism for improper assembly (10, 17, 18, 37). In contrast, we have achieved high levels of haploid induction using a *cenh3* mutation with a premature stop codon that is predicted to remove the sequence of the protein that interacts with other histones. The results suggest that quantitative reductions in CENH3 alone can induce centromere-mediated haploid induction, as predicted by the centromere size model (19). It is also possible that hypomorphic mutant alleles such as *cenh3-mu1015598* may induce haploids when crossed as heterozygotes, but this has yet to be tested.

One of the notable elements of centromere-mediated haploid induction is that it is effective in only a subset of progeny. In some individuals, all the chromosomes from the haploid-inducer parent are lost, and in another much larger subset, no chromosome loss occurs. The relatively small aneuploid class represents “partial haploid induction” events, where some chromosomes were lost but others survived. The fact that the *gl8* crosses yielded more true haploids than the *gl1* crosses may be related to the fact that the former were

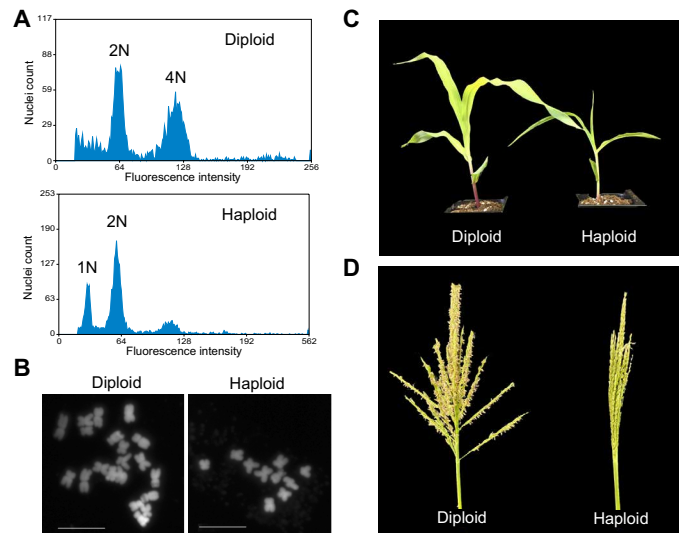


Fig. 2. Confirmation that plants are haploid. (A) Flow cytometric analysis of haploids. Diploid plants show peaks at 2N and 4N, where 4N is the result of endoreduplication in differentiated tissues. Haploid plants have 1N and 2N peaks. (B) Chromosome spreads. Maize diploids have 20 chromosomes, whereas haploids have 10. Scale bar, 20 μ m. (C) Haploids plants have a shorter stature. (D) Haploid plants are sterile without exerted anthers. Photo credit: Na Wang, University of Georgia.

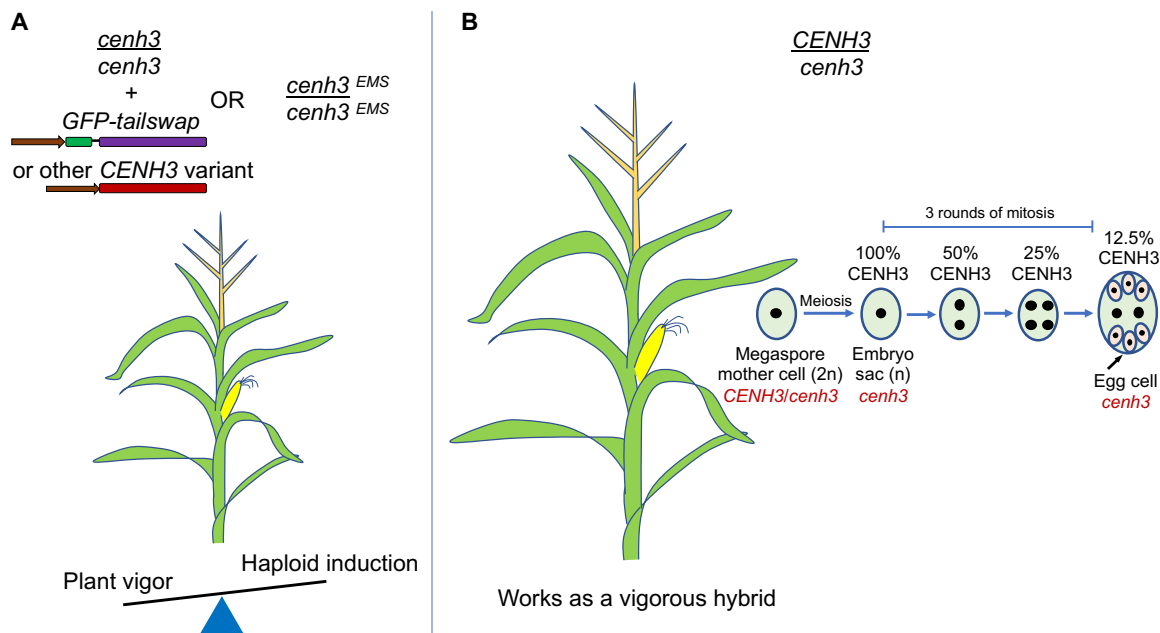


Fig. 3. Comparison of the GFP-tailswap-based method to the *cenh3* null method. (A) The GFP-tailswap method and its improved forms. In most applications, a transgene expressing a structurally altered CENH3, or other mutant form, is used to complement a loss-of-function mutation (10, 15, 17, 24). An EMS (ethyl methanesulfonate)-induced point mutation of native CENH3 has also been used (16). In all cases, the plant must grow to maturity with a partially dysfunctional CENH3 gene, which affects plant performance. The most effective haploid inducers are weak plants with poor fertility. (B) The *cenh3* null method. The plant is heterozygous and can be used as a vigorous hybrid. Haploid induction occurs at the gametophyte level. The female gametophyte is shown, where three mitotic cell divisions dilute CENH3 to low levels in the egg cell.

carried out in the summer, while the latter were carried out in winter. It is also possible that the selection scheme played a role. Studies using the maize *r-X1* deletion line, which generates monosomics at high frequency, have demonstrated that some chromosomes are recovered as monosomics at higher frequency than others (38). Monosomics for chromosome 5 (with *gl8*) are rarely recovered, whereas monosomics for chromosome 7 (with *gl1*) are far more common [17 times more common (38)]. Two of five sequenced aneuploids from *gl1* crosses were monosomic for chromosome 7 only (fig. S1). These data suggest that the *gl8* tester favors the recovery of haploids, while the *gl1* tester recovers both haploids and aneuploids.

It is likely that the frequency of haploid induction can be improved under standard breeding practices, similar to how the original ~3% haploid frequency observed with Stock 6 (1) was improved to ~15% in multiple breeding programs around the world (2). The major advantages of the *cenH3* approach are that it can be used to create either paternal or maternal haploids, that it does not require a transgene, and that the plants are phenotypically wild type and can be used as vigorous hybrids (Fig. 3). Since the inducer works as a heterozygote, *cenH3* can be crossed to any line, and the F1 will become a haploid inducer. This feature should make it particularly useful when combined with other technologies that are built upon haploids, such as genotype-independent gene editing (39) and synthetic apomixis (40).

METHODS

Plant materials

The *gl1*, *gl8*, and *cenH3-mu1015598* transposon insertion lines were obtained from the Maize Genetics Cooperation Stock Center, Urbana, IL. The *cenH3-mu1015598* allele is one of several mutations in the UFMu-01386 stock line. All plants were grown in the University of Georgia Plant Biology greenhouses. The *gl8* crosses were carried out in August of 2019, and the *gl1* crosses were carried out in December of 2019.

Construct preparation and transformation

The Ubi-Cas9 construct contains 1991 base pairs (bp) of the maize polyubiquitin promoter (GenBank, S94464.1) driving a maize codon-optimized version of Cas9 terminated by the NOS terminator. The *gRNA-ImmuneCENH3* construct contains two components, a *gRNA* module and the *ImmuneCENH3* gene. The *gRNA* portion contains the maize U6 promoter (41) driving a *gRNA* (TCCGCGACGCTACAGTCCC) terminated by the Pol III terminator TTTTTTTT. The *ImmuneCENH3* portion contains 6454 bp of the native *CENH3* gene (coordinates Chr6:166705239-166711693 on Zm-B73-REFERENCE-NAM-5.0) but has five silent codon changes in the *gRNA* target area (CCAGGTACGGTGCCTGCGCGA). The promoter includes 2184 bp of sequence upstream of the ATG.

To create the *gRNA-TailswapCENH3* construct, the natural 5'UTR of *CENH3* was retained, and a codon-optimized GFP sequence was inserted at the ATG of *ImmuneCENH3*. This was followed by a linker sequence ATGGATGAAGTATACAAGGGCGGAGGCGGTG-GAGGCGTCGAC and the tail sequence of the maize H3.3 gene (GenBank NM_001294303.2) including its intron, fused to the native *CENH3* gene 3-bp upstream of the *gRNA* target area. Our construct was based on the sequence of *Arabidopsis GFP-tailswap* obtained from the Comai laboratory.

Sequences of all three constructs are provided in the Supplementary Materials. The constructs were synthesized by GenScript (www.

genscript.com) and cloned into the binary vector pTF101.1 (42). The constructs were transformed into the maize HiII line at the Iowa State University Plant Transformation Facility (Ames, IA) and grown in the University of Georgia greenhouses. To generate the *cenH3* mutation, transgenic lines carrying *Ubi-Cas9* were crossed with lines carrying *gRNA-ImmuneCENH3*.

DNA extraction, genotyping, and sequence analysis

For standard leaf genotyping, genomic DNA was prepared using a CTAB (cetyl trimethylammonium bromide) protocol (43). Endosperm tissue was collected after the kernels had germinated and the glossy phenotype could be distinguished. Embryos and pericarps were removed with forceps, and the endosperm was ground to a powder with a mortar and pestle. The endosperm DNA was extracted with the IBI Plant Genomic DNA Mini Kit (IBI Scientific, IB47231).

To identify the presence of *ImmuneCENH3* and Cas9 in transgenic lines, primers CENH3-F2 and CENH3-R3 were used to amplify *ImmuneCENH3*, and primers Cas9-F1 and Cas9-R1 were used to amplify Cas9 (table S3). To identify the original *cenH3* mutation in Cas9 plants, polymerase chain reaction (PCR) was carried out using the Phusion High-Fidelity PCR Kit (New England Biolabs, Ipswich, MA) with primers CENH3-F1 and CENH3-R1 in table S3. The PCR products were either directly Sanger sequenced or cloned using a TOPO TA cloning kit (Thermo Fisher Scientific, #K457501) and then Sanger sequenced.

In lines that lack *ImmuneCENH3*, the *cenH3* null allele was differentiated from the native *CENH3* allele by PCR and restriction enzyme digestion. PCR amplifies a 496-bp PCR product using primers CENH3-F2 and CENH3-R2. When this product is digested with the restriction endonuclease AlwNI (New England Biolabs), the wild-type allele is cleaved into two pieces of size 284 and 212 bp, while the mutant *cenH3* allele is not cleaved.

The *cenH3-mu1015598* allele was scored using the primers CENH3-F4, CENH3-R4, and Mumix (a 1:1 mix of the two primers EoMu1 and EoMu2 in table S3). The wild-type allele is amplified with CENH3-F4 and CENH3-R4, while the *Mu* allele is amplified with CENH3-F4 and Mumix.

Ploidy evaluation

Progeny from *+cenH3* crosses were grown indoors under grow lights for 10 to 13 days and water sprayed on the seedlings to identify the glossy phenotype. All glossy plants were subsequently assayed by flow cytometry. For each individual, about 1 g of flash-frozen leaves or roots were collected and finely chopped with a razor blade in 1.5 ml of prechilled nuclei extraction buffer [2 mM EDTA, 15 mM tris-HCl (pH 7.5), 20 mM NaCl, 80 mM KCl, 0.5 mM spermine, 15 mM 2-mercaptoethanol, 0.1 mM phenylmethylsulfonyl fluoride, and 0.1% Triton X-100]. After chopping, the mixture was filtered twice through a 40- μ m cell strainer (pluriSelect, 43-10040-60). The nuclei were stained with 4,6-diamidino-2-phenylindole (DAPI) and loaded into flow cytometers hosted by the CTEGD Cytometry Shared Resource Lab at the University of Georgia.

Chromosome spreads

Chromosome analysis was carried out as described in (44). Briefly, root tips were collected from the haploid and diploid plants, incubated in a chamber with nitrous oxide for 3 hours, and fixed with 90% acetic acid. Root tips were cut with a razor blade and digested in an enzyme solution (1% pectolyase Y-23 and 2% cellulase Onozuka

R-10) at 37°C for 50 min. The root section was washed in ethanol and then immersed in 90% acetic acid. A metal pick was used to crush the roots tips, and 10 µl of the cell suspension was dropped onto microscope slides. Slides were dried and mounted with a glass coverslip using ProLong Gold with DAPI (Thermo Fisher Scientific, catalog no. P36931). Slides were imaged on a Zeiss Axio Imager M1 fluorescence microscope with a 63× Plan-Apochromat oil objective, and SlideBook software (Intelligent Imaging Innovations, Denver, CO, USA) was used to analyze the data.

Skim sequencing of haploids and aneuploids

For each sample, DNA (12 ng/µl) was sonicated in a 100-µl volume with a Diagenode Bioruptor for 7 min on high setting with 30-s on-off intervals, yielding fragments averaging about 500 bp in length. DNA sequencing libraries were prepared using the KAPA HyperPrep Kit (KK8502) with KAPA single-indexed adapters (KK8700). Six hundred nanograms of sonicated DNA was used as input for each sample, and three cycles of PCR were used to amplify libraries. One hundred fifty-nucleotide Illumina sequencing reads were adapter-trimmed and quality-filtered using Cutadapt version 1.9.1 (45) with parameters as follows: “-q 20 -a AGATCGGAAGAGC -e .05 -O 1 -m 50.” Reads were aligned to Zm-B73-REFERENCE-NAM-5.0 (<https://nam-genomes.org/>) using BWA-MEM version 0.7.15 in single-end mode with default parameters (46). Read coverage was visualized using IGVTools version 2.3.98 (47) with coverage calculated on 25-Mb intervals. Raw sequence data are available in the National Center for Biotechnology Information (NCBI) BioProject database under accession number PRJNA646652.

SUPPLEMENTARY MATERIALS

Supplementary material for this article is available at <http://advances.sciencemag.org/cgi/content/full/7/4/eabe2299/DC1>

[View/request a protocol for this paper from Bio-protocol.](#)

REFERENCES AND NOTES

- E. H. Coe Jr., A line of maize with high haploid frequency. *Am. Nat.* **93**, 381–382 (1959).
- H. U. Trentin, U. K. Frei, T. Lübberstedt, Breeding maize maternal haploid inducers. *Plant Theory* **9**, 614 (2020).
- T. Kelliher, D. Starr, L. Richbourg, S. Chintamanani, B. Delzer, M. L. Nuccio, J. Green, Z. Chen, J. McCuiston, W. Wang, T. Liebler, P. Bullock, B. Martin, MATRILINEAL, a sperm-specific phospholipase, triggers maize haploid induction. *Nature* **542**, 105–109 (2017).
- C. Liu, X. Li, D. Meng, Y. Zhong, C. Chen, X. Dong, X. Xu, B. Chen, W. Li, L. Li, X. Tian, H. Zhao, W. Song, H. Luo, Q. Zhang, J. Lai, W. Jin, J. Yan, S. Chen, A 4-bp insertion at ZmPLA1 encoding a putative phospholipase generates haploid induction in maize. *Mol. Plant* **10**, 520–522 (2017).
- L. M. Gilles, A. Khaled, J.-B. Laffaire, S. Chaignon, G. Gendrot, J. Laplaige, H. Bergès, G. Beydon, V. Bayle, P. Barret, J. Comadran, J.-P. Martinant, P. M. Rogowsky, T. Wiedez, Loss of pollen-specific phospholipase NOT LIKE DAD triggers gynogenesis in maize. *EMBO J.* **36**, 707–717 (2017).
- L. Yao, Y. Zhang, C. Liu, Y. Liu, Y. Wang, D. Liang, J. Liu, G. Sahoo, T. Kelliher, OsmATL mutation induces haploid seed formation in indica rice. *Nat. Plants* **4**, 530–533 (2018).
- H. Liu, K. Wang, Z. Jia, Q. Gong, Z. Lin, L. Du, X. Pei, X. Ye, Efficient induction of haploid plants in wheat by editing of TaMTL using an optimized Agrobacterium-mediated CRISPR system. *J. Exp. Bot.* **71**, 1337–1349 (2020).
- C. Liu, Y. Zhong, X. Qi, M. Chen, Z. Liu, C. Chen, X. Tian, J. Li, Y. Jiao, D. Wang, Y. Wang, M. Li, M. Xin, W. Liu, W. Jin, S. Chen, Extension of the *in vivo* haploid induction system from diploid maize to hexaploid wheat. *Plant Biotechnol. J.* **18**, 316–318 (2020).
- Y. Zhong, B. Chen, M. Li, D. Wang, Y. Jiao, X. Qi, M. Wang, Z. Liu, C. Chen, Y. Wang, M. Chen, J. Li, Z. Xiao, D. Cheng, W. Liu, K. Boutilier, C. Liu, S. Chen, A DMP-triggered *in vivo* maternal haploid induction system in the dicotyledonous *Arabidopsis*. *Nat. Plants* **6**, 466–472 (2020).
- M. Ravi, S. W. L. Chan, Haploid plants produced by centromere-mediated genome elimination. *Nature* **464**, 615–618 (2010).
- D. K. Palmer, K. O'Day, M. H. Wener, B. S. Andrews, R. L. Margolis, A 17-kD centromere protein (CENP-A) copurifies with nucleosome core particles and with histones. *J. Cell Biol.* **104**, 805–815 (1987).
- C. X. Zhong, J. B. Marshall, C. Topp, R. Mroczek, A. Kato, K. Nagaki, J. A. Birchler, J. Jiang, R. K. Dawe, Centromeric retroelements and satellites interact with maize kinetochore protein CENH3. *Plant Cell* **14**, 2825–2836 (2002).
- K. Kixmoeller, P. K. Allu, B. E. Black, The centromere comes into focus: From CENP-A nucleosomes to kinetochore connections with the spindle. *Open Biol.* **10**, 200051 (2020).
- A. Musacchio, A. Desai, A molecular view of kinetochore assembly and function. *Biology* **6**, 5 (2017).
- R. Karimi-Ashtiyani, T. Ishii, M. Niessen, N. Stein, S. Heckmann, M. Gurushidze, A. M. Banaei-Moghaddam, J. Fuchs, V. Schubert, K. Koch, O. Weiss, D. Demidov, K. Schmidt, J. Kumlehn, A. Houben, Point mutation impairs centromeric CENH3 loading and induces haploid plants. *Proc. Natl. Acad. Sci. U.S.A.* **112**, 11211–11216 (2015).
- S. Kuppu, E. H. Tan, H. Nguyen, A. Rodgers, L. Comai, S. W. L. Chan, A. B. Britt, Point mutations in centromeric histone induce post-zygotic incompatibility and uniparental inheritance. *PLOS Genet.* **11**, e1005494 (2015).
- S. Kuppu, M. Ron, M. P. A. Marimuthu, G. Li, A. Huddleson, M. H. Siddeek, J. Terry, R. Buchner, N. Shabek, L. Comai, A. B. Britt, A variety of changes, including CRISPR/Cas9 mediated deletions, in CENH3 lead to haploid induction on outcrossing. *Plant Biotechnol. J.* **18**, 2068–2080 (2020).
- K. Kalinowska, S. Chamas, K. Unkel, D. Demidov, I. Lermontova, T. Dresselhaus, J. Kumlehn, F. Dunemann, A. Houben, State-of-the-art and novel developments of *in vivo* haploid technologies. *Theor. Appl. Genet.* **132**, 593–605 (2019).
- N. Wang, R. Kelly Dawe, Centromere size and its relationship to haploid formation in plants. *Mol. Plant* **11**, 398–406 (2018).
- M. Ravi, F. Shibata, J. S. Ramahi, K. Nagaki, C. Chen, M. Murata, S. W. L. Chan, Meiosis-specific loading of the centromere-specific histone CENH3 in *Arabidopsis thaliana*. *PLOS Genet.* **7**, e1002121 (2011).
- T. Kelliher, D. Starr, W. Wang, J. McCuiston, H. Zhong, M. L. Nuccio, B. Martin, Maternal haploids are preferentially induced by CENH3-tailswap transgenic complementation in maize. *Front. Plant Sci.* **7**, 414 (2016).
- C. Feng, J. Yuan, H. Bai, Y. Liu, H. Su, Y. Liu, L. Shi, Z. Gao, J. A. Birchler, F. Han, The deposition of CENH3 in maize is stringently regulated. *Plant J.* **102**, 6–17 (2019).
- A. Barkan, R. A. Martienssen, Inactivation of maize transposon Mu suppresses a mutant phenotype by activating an outward-reading promoter near the end of Mu1. *Proc. Natl. Acad. Sci. U.S.A.* **88**, 3502–3506 (1991).
- S. Maheshwari, E. H. Tan, A. West, F. C. H. Franklin, L. Comai, S. W. L. Chan, Naturally occurring differences in CENH3 affect chromosome segregation in zygotic mitosis of hybrids. *PLOS Genet.* **11**, e1004970 (2015).
- D. L. Bodor, J. F. Mata, M. Sergeev, A. F. David, K. J. Salimian, T. Panchenko, D. W. Cleveland, B. E. Black, J. V. Shah, L. E. Jansen, The quantitative architecture of centromeric chromatin. *eLife* **3**, e02137 (2014).
- N. Raychaudhuri, R. Dubruielle, G. A. Orsi, H. C. Bagheri, B. Loppin, C. F. Lehner, Transgenerational propagation and quantitative maintenance of paternal centromeres depends on Cid/Cenp-A presence in *Drosophila* sperm. *PLoS Biol.* **10**, e1001434 (2012).
- I. Lermontova, V. Schubert, J. Fuchs, S. Klatte, J. Macas, I. Schubert, Loading of *Arabidopsis* centromeric histone CENH3 occurs mainly during G2 and requires the presence of the histone fold domain. *Plant Cell* **18**, 2443–2451 (2006).
- S. S. Chase, Monoploids and monoploid-derivatives of maize (*Zea mays* L.). *Bot. Rev.* **35**, 117–168 (1969).
- M. Ravi, M. P. A. Marimuthu, E. H. Tan, S. Maheshwari, I. M. Henry, B. Marin-Rodriguez, G. Urtecho, J. Tan, K. Thornhill, F. Zhu, A. Panoli, V. Sundaresan, A. B. Britt, L. Comai, S. W. L. Chan, A haploid genetics toolbox for *Arabidopsis thaliana*. *Nat. Commun.* **5**, 5334 (2014).
- E. H. Tan, I. M. Henry, M. Ravi, K. R. Bradnam, T. Mandakova, M. P. Marimuthu, I. Korf, M. A. Lysak, L. Comai, S. W. Chan, Catastrophic chromosomal restructuring during genome elimination in plants. *eLife* **4**, e06516 (2015).
- Y. Li, G. Segal, Q. Wang, H. K. Dooner, Gene tagging with engineered Ds elements in maize. *Methods Mol. Biol.* **1057**, 83–99 (2013).
- T. Ishii, R. Karimi-Ashtiyani, A. Houben, Haploidization via chromosome elimination: Means and mechanisms. *Annu. Rev. Plant Biol.* **67**, 421–438 (2016).
- A. Iwata-Otsubo, J. M. Dawicki-McKenna, T. Aker, S. J. Falk, L. Chmátal, K. Yang, B. A. Sullivan, R. M. Schultz, M. A. Lampson, B. E. Black, Expanded satellite repeats amplify a discrete CENP-A nucleosome assembly site on chromosomes that drive in female meiosis. *Curr. Biol.* **27**, 2365–2373.e8 (2017).
- T. Aker, E. Trimm, M. A. Lampson, Molecular strategies of meiotic cheating by selfish centromeres. *Cell* **178**, 1132–1144.e10 (2019).

35. S. Henikoff, K. Ahmad, H. S. Malik, The centromere paradox: Stable inheritance with rapidly evolving DNA. *Science* **293**, 1098–1102 (2001).
36. J. D. Brown, R. J. O'Neill, Chromosomes, conflict, and epigenetics: Chromosomal speciation revisited. *Annu. Rev. Genomics Hum. Genet.* **11**, 291–316 (2010).
37. A. B. Britt, S. Kupp, CenH3: An emerging player in haploid induction technology. *Front. Plant Sci.* **7**, 357 (2016).
38. D. F. Weber, in *The Maize Handbook*, M. Freeling, V. Walbot, Eds. (Springer New York, 1994), pp. 350–358.
39. T. Kelliher, D. Starr, X. Su, G. Tang, Z. Chen, J. Carter, P. E. Wittich, S. Dong, J. Green, E. Burch, J. McCuiston, W. Gu, Y. Sun, T. Strebe, J. Roberts, N. J. Bate, Q. Que, One-step genome editing of elite crop germplasm during haploid induction. *Nat. Biotechnol.* **37**, 287–292 (2019).
40. C. Wang, Q. Liu, Y. Shen, Y. Hua, J. Wang, J. Lin, M. Wu, T. Sun, Z. Cheng, R. Mercier, K. Wang, Clonal seeds from hybrid rice by simultaneous genome engineering of meiosis and fertilization genes. *Nat. Biotechnol.* **37**, 283–286 (2019).
41. S. Svitashchev, J. K. Young, C. Schwartz, H. Gao, S. C. Falco, A. M. Cigan, Targeted mutagenesis, precise gene editing, and site-specific gene insertion in maize using Cas9 and guide RNA. *Plant Physiol.* **169**, 931–945 (2015).
42. M. M. Paz, H. Shou, Z. Guo, Z. Zhang, A. K. Banerjee, K. Wang, Assessment of conditions affecting Agrobacterium-mediated soybean transformation using the cotyledonary node explant. *Euphytica* **136**, 167–179 (2004).
43. J. D. Clarke, Cetyltrimethyl ammonium bromide (CTAB) DNA miniprep for plant DNA isolation. *Cold Spring Harb. Protoc.* **2009**, pdb.prot4981 (2009).
44. R. K. Dawe, E. G. Lowry, J. I. Gent, M. C. Stitzer, K. W. Swentowsky, D. M. Higgins, J. Ross-Ibarra, J. G. Wallace, L. B. Kanizay, M. Alabady, W. Qiu, K.-F. Tseng, N. Wang, Z. Gao, J. A. Birchler, A. E. Harkess, A. L. Hodges, E. N. Hiatt, A kinesin-14 motor activates neocentromeres to promote meiotic drive in maize. *Cell* **173**, 839–850.e18 (2018).
45. M. Martin, Cutadapt removes adapter sequences from high-throughput sequencing reads. *EMBnet.journal* **17**, 10 (2011).
46. H. Li, R. Durbin, Fast and accurate short read alignment with Burrows-Wheeler transform. *Bioinformatics* **25**, 1754–1760 (2009).
47. H. Thorvaldsdóttir, J. T. Robinson, J. P. Mesirov, Integrative genomics viewer (IGV): High-performance genomics data visualization and exploration. *Brief. Bioinform.* **14**, 178–192 (2013).

Acknowledgments: We thank M. Tindall Smith, F. Fu, and S. Greenlaw for help with genotyping, W. A. Ricci for help with the flow cytometry analysis, and J. Liu for critically reading the manuscript. We appreciate the support of the Georgia Genomics and Bioinformatics Core facility, the UGA Cytometry Shared Resource Laboratory, and the Georgia Advanced Computing Resource Center. **Funding:** This work was funded by grant 1444514 from the NSF. **Author contributions:** R.K.D. supervised the research. N.W. and J.I.G. performed the experiments. N.W. and R.K.D. prepared the figures. N.W., J.I.G., and R.K.D. wrote the paper. **Competing interests:** R.K.D. is an inventor on provisional patents related to this work filed by the University of Georgia (numbers 63/036,902 and 63/036,910, filed 9 June 2020). The other authors declare that they have no competing interests. **Data and materials availability:** Sequence data are available in the NCBI BioProject database under accession number PRJNA646652. Seeds carrying the *cenH3* null mutation can be obtained from the corresponding author under a University of Georgia material transfer agreement. All data needed to evaluate the conclusions in the paper are present in the paper and/or the Supplementary Materials. Additional data related to this paper may be requested from the authors.

Submitted 7 August 2020
Accepted 5 November 2020
Published 20 January 2021
10.1126/sciadv.abe2299

Citation: N. Wang, J. I. Gent, R. K. Dawe, Haploid induction by a maize *cenH3* null mutant. *Sci. Adv.* **7**, eabe2299 (2021).

Haploid induction by a maize *cenh3* null mutant

Na Wang, Jonathan I. Gent and R. Kelly Dawe

Sci Adv 7 (4), eabe2299.

DOI: 10.1126/sciadv.abe2299

ARTICLE TOOLS

<http://advances.sciencemag.org/content/7/4/eabe2299>

SUPPLEMENTARY MATERIALS

<http://advances.sciencemag.org/content/suppl/2021/01/14/7.4.eabe2299.DC1>

REFERENCES

This article cites 45 articles, 8 of which you can access for free
<http://advances.sciencemag.org/content/7/4/eabe2299#BIBL>

PERMISSIONS

<http://www.sciencemag.org/help/reprints-and-permissions>

Use of this article is subject to the [Terms of Service](#)

Science Advances (ISSN 2375-2548) is published by the American Association for the Advancement of Science, 1200 New York Avenue NW, Washington, DC 20005. The title *Science Advances* is a registered trademark of AAAS.

Copyright © 2021 The Authors, some rights reserved; exclusive licensee American Association for the Advancement of Science. No claim to original U.S. Government Works. Distributed under a Creative Commons Attribution NonCommercial License 4.0 (CC BY-NC).